Automatic Modulation Classification via Instantaneous Features

Elliott Moser[1], Michael K. Moran[2], Erric Hillen[3], Dong Li[3] and Zhiqiang Wu[3]
[1]MacAulay Brown, Inc.
[2]Sensors Directorate, Air Force Research Laboratory
[3]Department of Electrical Engineering, Wright State University

***Abstract*—Automatic modulation classification has attracted a lot of interests in the research community in recent years due to the advances in cognitive RF signal processing such as cognitive radio, cognitive radar and cognitive electronic warfare. There are two major approaches in automatic modulation classification, namely the feature based approach and the decision theoretic approach. In our previous work, we have demonstrated the feasibility of using cyclostationary statistical features such as spectrum correlation function to perform modulation detection and classification for both RF signals and underwater acoustic signals. In this paper, we try to develop automatic modulation classification algorithms employing instantaneous features such as instantaneous amplitude, phase and frequency parameters. By extending previously developed features and evaluating appropriate decision metrics, we have been able to expand our modulation classification capability to 9 popular modulations including 2ASK, 4ASK, 8ASK, 2FSK, 4FSK, 8FSK and 2PSK, 4PSK, 8PSK. Thorough simulation results confirm the effectiveness of our proposed algorithm and threshold choices. The success of this approach also suggests a future research direction to combine statistical features with instantaneous features to provide a more accurate and more robust modulation identification algorithm.**

KEYWORDS

Automatic Modulation Classification, AMC, Digital Modulation, Instantaneous Information

I. Introduction

Automatic Modulation Classification (AMC) is a class of techniques for recognizing the type of digital modulation scheme used to generate a received modulated signal, with little or even no prior knowledge (such as its phase, frequency or amplitude) about the modulated signal itself [1]; and plays a key role in various civilian and military applications. With recent advances in cognitive RF technologies such as cognitive radio and dynamic spectrum access network, cognitive radar, and cognitive electronic warfare (EW), automatic modulation classification has attracted a lot of interests in the research community in recent years.

The spectrum of these signals may range from high frequency (HF) to very high frequency (VHF), and their format can vary from simple narrowband modulations to wideband schemes. Under such conditions, advanced techniques are required for real-time signal interception and processing, which are vital for decisions involving electronic warfare operations and other tactical actions. Furthermore, in the past, COMINT systems generally relied on operator interpretations of measured parameters of intercepted signals to distinguish modulation type, however, with the increasing set of modulation schemes, as well as, the increase processing power of today's systems, automatic modulation schemes are becoming more valuable than manual modulation identification [2].

AMC algorithms can be separated into two categories, likelihood-based (LB) [3]–[7]and feature-based (FB) [2], [8]–[14] methods, respectively. LB methods have two steps: calculating the likelihood function of the received signal for all candidate modulations, and then using maximum likelihood ratio test for decision making. LB algorithms are optimal classifiers, however, suffer from computational complexity. In the FB approach several features are extracted from the received signal and then applied to a classifier in order to recognize the modulation type. Although FB-based methods may not be optimal, they are usually simple to implement, with near-optimal performance, when designed properly.

In our previous work, we have demonstrated how to use statistical likelihood approach to perform automatic modulation classifications. Such statistical features include spectral correlation function (SCF), spectral coherence function (SOF) and fourth-order cumulants [15]–[27]. We have successfully applied these features to RF signals and underwater acoustic signals and developed corresponding classification algorithms to perform modulation classification accurately.

In this paper, we try to conduct research in automatic modulation classification through instantaneous features such as instantaneous amplitude, phase and frequency parameters. Built upon the features proposed by reference [2], we expand their algorithm into a hierarchical modulation classifier with more layers. As a direct result, we have been able to classify more modulation types. Specifically, we are able to classify 9 commonly used modulation types: 2ASK, 4ASK, 2FSK, 4FSK, 2PSK, 4PSK, as well as 8ASK, 8FSK, and 8PSK. Simulations over different signal to noise ratios confirm the effectiveness of the algorithm and the choice of thresholds.

The remaining part of this paper is organized as follows. In Section II, we briefly describe the system model and review the instantaneous features used for automatic modulation detection. In Section III, we present the extended hierarchical modulation classifier and associated threshold determination algorithm. Section IV provides numerical results of the performance of the proposed automatic modulation classifier.

Conclusion follows.

II. System Model and Instantaneous Features

In the system model, we assume that an intercepted radio frequency signal of K seconds is sampled at sampling rate f_s and is divided into M successive frames each with N samples, $M(= Kf_s/N)$ frames. Next, from every available frame we decide what type of modulation it is. Finally, once a decision for all frames is made, the use of majority logic rule is applied; i.e. select the decision with the largest number of repetitions.

1) Key Features: When determining modulation type of an intercepted signal, we use the same five key features as in [2] based on instantaneous amplitude, phase, and frequency, to determine the modulation type. The intercepted signal $x(t)$ can be represented as the analytic signal $z(t)$, which is expressed as

$$z(t) = x(t) + jy(t), \tag{1}$$

where $y(t)$ is the Hilbert transform of $x(t)$, and j is the imaginary unit. From the analytic signal one can determine the instantaneous amplitude, phase, and frequency. The instantaneous amplitude $A(t)$ is given by

$$A(t) = |z(t)| = \sqrt{x^2(t) + y^2(t)}. \tag{2}$$

The instantaneous phase $\phi(t)$ is given by

$$\phi(t) = \arg\{z(t)\} = \arctan\left(\frac{y(t)}{x(t)}\right) \tag{3}$$

The instantaneous frequency $f(t)$ is given by

$$f(t) = \frac{1}{2\pi}\frac{d\phi_{uw}(t)}{dt} \tag{4}$$

where ϕ_{uw} is the unwrapped instantaneous phase [28].

From here, the five key features are defined. The first key feature, γ_{max}, represents the maximum value of the spectral power density of the normalized-centered instantaneous amplitude of the intercepted signal and is defined by

$$\gamma_{max} = \frac{\max|DFT(A_{cn}(i))|^2}{N} \tag{5}$$

where $A_{cn}(i)$ is the normalized-centered instantaneous amplitude at time instants $t = i/f_s (i = 1, 2, ..., N)$ and it is defined by

$$A_{cn}(i) = A_n(i) - 1, A_n(i) = \frac{A(i)}{m_a} \tag{6}$$

where m_a is the average value of the instantaneous amplitude over one frame.

$$m_a = \frac{1}{N}\sum_{i=1}^{N} A(i) \tag{7}$$

and N is the number of samples for that segment. There is a slight modification to (5) from [2], in that it is divided by the number of samples in the segment.

The next key feature, σ_{ap}, represents the standard deviation of the absolute value of the non-linear component of the instantaneous phase, evaluated over the non-weak segments of the intercepted signal and is defined by

$$\sigma_{ap} = \sqrt{\frac{1}{C}\left(\sum_{A_n(i)>a_t} \phi_{NL}^2(i)\right) - \left(\frac{1}{C}\sum_{A_n(i)>a_t} |\phi_{NL}(i)|\right)^2} \tag{8}$$

where $\phi_{NL}(i)$ is the non-linear component of the instantaneous phase,

$$\phi_{NL}(i) = \phi_{uw} - \frac{2\pi f_c i}{f_s} \tag{9}$$

C is the number of samples in $\{\phi(i)\}$ for which $A_n(i) > a_t$, and a_t is a threshold for $A(t)$ below which the estimation of the instantaneous phase is very sensitive to noise.

The third key feature, σ_{dp}, represents the standard deviation of the non-linear component of the direct, not absolute, instantaneous phase, evaluated over the non-weak segments of the signal and is defined by

$$\sigma_{dp} = \sqrt{\frac{1}{C}\left(\sum_{A_n(i)>a_t} \phi_{NL}^2(i)\right) - \left(\frac{1}{C}\sum_{A_n(i)>a_t} \phi_{NL}(i)\right)^2} \tag{10}$$

The fourth key feature, σ_{aa}, represents the standard deviation of the absolute value of the normalized-centered instantaneous amplitude of the signal and is defined by

$$\sigma_{aa} = \sqrt{\frac{1}{N}\left(\sum_{i=1}^{N} A_{cn}^2(i)\right) - \left(\frac{1}{N}\sum_{i=1}^{N} |A_{cn}(i)|\right)^2} \tag{11}$$

The final key feature, σ_{fa}, represents the standard deviation of the absolute value of the normalized-centered instantaneous frequency, evaluated over the non-weak segments of the intercepted signal and is defined by

$$\sigma_{fa} = \sqrt{\frac{1}{C}\left(\sum_{A_n(i)>a_t} f_N^2(i)\right) - \left(\frac{1}{C}\sum_{A_n(i)>a_t} |f_N(i)|\right)^2} \tag{12}$$

where

$$\begin{aligned} f_N(i) &= f_c(i)/rb, \\ f_c(i) &= f(i) - m_f \\ m_f &= \frac{1}{N}\sum_{i=1}^{N} f(i), \end{aligned} \tag{13}$$

and r_b is the bit rate.

The choice of γ_{max}, σ_{ap}, σ_{dp}, σ_{aa}, and σ_{fa} as key features in [2] are based on the following facts:

- γ_{max} is used to discriminate 2FSK and 4FSK signals from 2ASK, 4ASK, 2PSK, and 4PSK signals. 2FSK and 4FSK signals have constant instantaneous amplitude, thereby, their normalized-centered instantaneous amplitude is zero. Furthermore, their spectral power densities are zero, meaning the two signal types have no amplitude information. 2ASK and 4ASK do not have constant instantaneous amplitudes, therefore, they possess amplitude information. Finally, 2PSK and 4PSK signals have amplitude information due to bandlimitation imposing amplitude information.

- σ_{ap} is used to discriminate 2ASK, 4ASK, and 2PSK signals from a 4PSK signal. 2ASK and 4ASK signals have no absolute phase information by their nature. Also, it is well established that the direct phase of 2PSK signals takes on values of 0 and π, so its absolute value after centering is constant ($= \pi/2$) such that is has no absolute phase information. A 4PSK signal, by its nature, has absolute and direct phase information.
- σ_{dp} is used to discriminate 2ASK and 4ASK signals from a 2PSK signal. 2ASK and 4ASK signals have no direct phase information by their nature. A 2PSK signal, however, does have direct phase information by its nature (the instantaneous phase takes on values of 0 and π).
- σ_{aa} is used to discriminate a 2ASK signal from a 4ASK signal, because the normalized-centered instantaneous amplitude of a 2ASK signal is changed between two levels (± 1) so its absolute value is constant, thereby has no absolute amplitude information. A 4ASK signal has both absolute and direct amplitude information, by its nature.
- σ_{fa} is used to discriminate a 2FSK signal from a 4FSK signal because the normalized instantaneous frequency of a 2FSK signal changes between two levels (± 1) so its absolute value is constant, thereby, it has no absolute frequency information. A 4FSK signal has absolute and direct frequency information by its nature.

III. Extended Automatic Modulation Classifier

Now we propose an extended automatic modulation classifier to include 8ASK, 8FSK, and 8PSK. We first develop the appropriate modulation parameters with the additional modulation types as shown in Table I. Next, we run a test simulation to acquire Key Feature vs SNR curves. Figures 1-5 show the resulting plots for the extension into 8ASK, 8PSK, and 8FSK for N = 8192.

TABLE I
Digitally Modulated Signals parameters selection

Modulation Type	M	a_θ	f_θ (kHz)	ϕ_θ
MASK	2	$0.8\theta + 0.2$	f_c	0
	4	$0.25\theta + 0.25$	f_c	0
	8	$0.125\theta + 0.125$	f_c	0
MPSK	2	1	f_c	$(1-\theta)\pi$
	4	1	f_c	$\theta(\pi/2)$
	8	1	f_c	$\theta(\pi/4)$
MFSK	2	1	$4r_b\theta + f_c - 2r_b$	0
	4	1	$\frac{f_c-(\theta+1)r_b if \theta<2}{f_c+(\theta-1)r_b if \theta\geq 2}$	0
	8	1	$\frac{f_c-(\theta+1)r_b if \theta<4}{f_c+(\theta-3)r_b if \theta\geq 4}$	0

Upon looking at the resulting figures it becomes apparent that a new scheme and additional thresholds needs to be determined. First and foremost, much of the decision theoretic stays the same, however, with the addition of M = 8 modulations and maintaining the same key features, a second set of thresholds

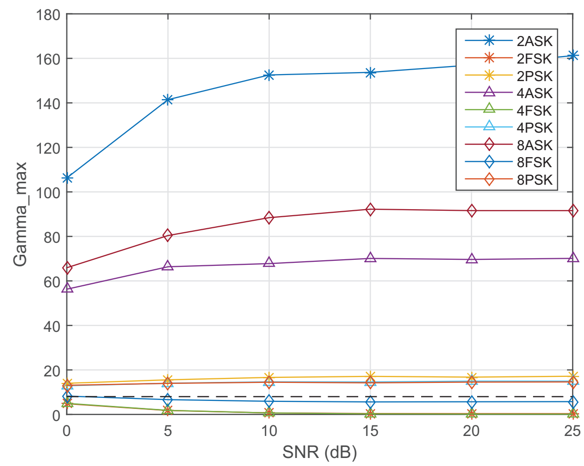

Fig. 1. Dependence of γ_{max} on SNR (8192).

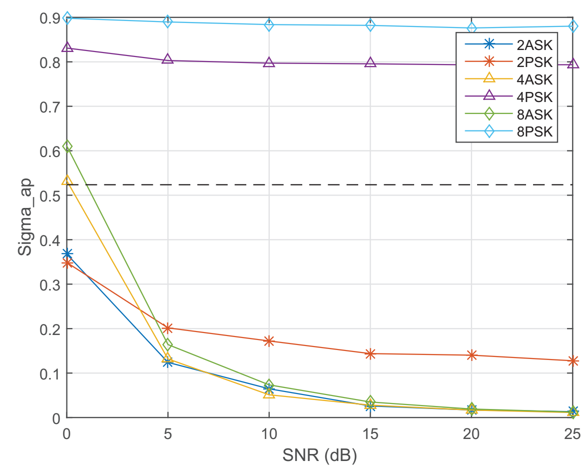

Fig. 2. Dependence of σ_{ap} on SNR (8192).

is chosen to accurately distinguish between the modulation types. Figure 6 provides the new scheme.

The thresholds remain the same as before, except for $t_{\gamma_{max}}$ being increased to 8 to allow 8FSK to be correctly identified, with the addition of three new thresholds, $t_{\sigma_{ap2}}$, $t_{\sigma_{aa2}}$, and $t_{\sigma_{fa2}}$. $t_{\sigma_{ap2}}$ distinguishes 4PSK from 8PSK; $t_{\sigma_{aa2}}$ distinguishes 4ASK from 8ASK; and $t_{\sigma_{fa2}}$ distinguishes 4FSK from 8FSK. The chosen thresholds, $t_{\gamma_{max}}$, $t_{\sigma_{ap}}$, $t_{\sigma_{ap2}}$, $t_{\sigma_{dp}}$, $t_{\sigma_{aa}}$, $t_{\sigma_{aa2}}$, $t_{\sigma_{fa}}$, and $t_{\sigma_{fa2}}$ are 8, pi/6, 0.85, pi/3, 0.2, 0.24, 0.52, and 0.7, respectively.

IV. Numerical Results

Using MatLab 2014b, we generate 400 realizations for the three additional modulation types using the parameters from Table I. Next, AWGN is added to each signal for SNR values of 10 and 20 dB and is band-limited by being passed through a bandpass filter using the appropriate bandwidths. Each set of realizations are stored into a separate .mat file and are

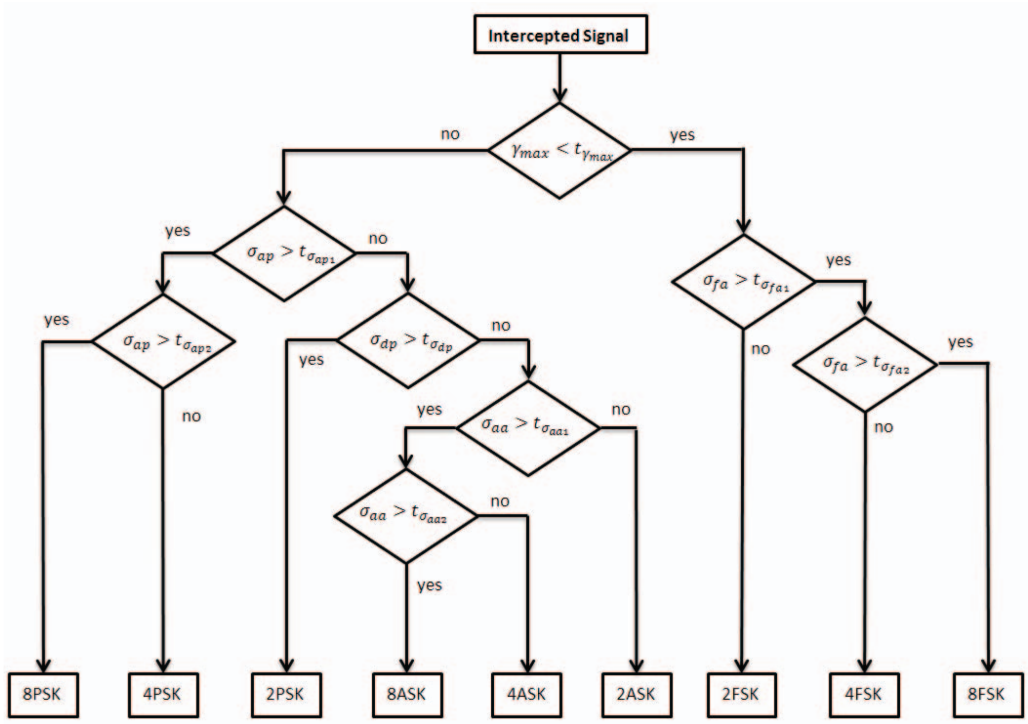

Fig. 6. Flowchart for extended automatic identification of digital modulations

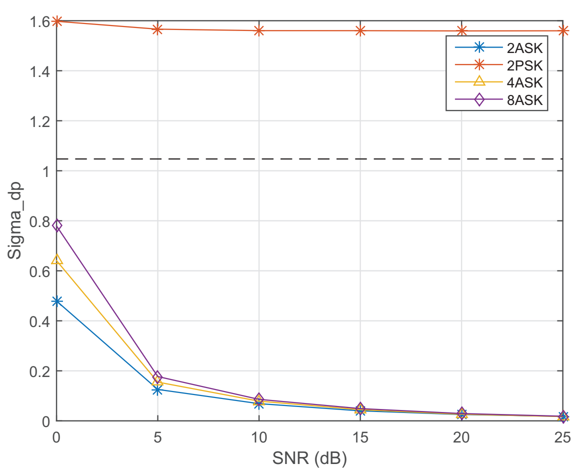

Fig. 3. Dependence of σ_{dp} on SNR (8192).

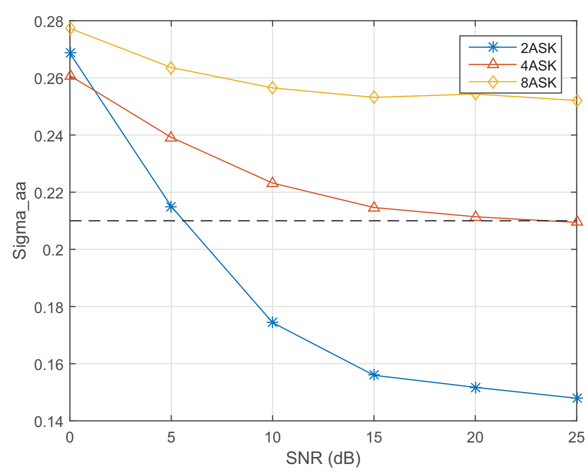

Fig. 4. Dependence of σ_{aa} on SNR (8192).

of 1 second duration. In total there are now 18 data sets, 9 associated with SNR of 10 dB and 9 associated with SNR of 20 dB.

Next, using the new scheme from Figure 6 and new thresholds we run the algorithm and obtain a confusion matrix for N = 2048 and N = 8192 at SNR = 10 dB and SNR = 20 dB, provided in Tables II-V

2) Results with New Thresholds for $N = 2048$: Our first simulation with the addition of 8ASK, 8FSK, and 8PSK returns to the $N = 2048$ sample case. Simulations are performed to 400 realizations at 10 dB and 20 dB SNR with our newly established thresholds that include consideration of the new modulation schemes.

The results of the first set of the simulations are shown in Tables II and III. In the 10 dB SNR simulation, we observe that all ASK modulation schemes are properly identified in 100% of simulations. For FSK, 4FSK and 8FSK are correctly identified in most simulations, whereas 2FSK is nearly always mis-identified as 8FSK. Finally, in this set of simulations, PSK is not correctly identified at all, with 2PSK mostly identified

TABLE II
N = 2048 WITH NEW THRESHOLDS AND EXTENSION

Digital Modulation Recognition procedure at SNR = 10 dB									
Modulation Type	Deduced Modulation Type								
	2ASK	4ASK	8ASK	2FSK	4FSK	8FSK	2PSK	4PSK	8PSK
2ASK	100%	-	-	-	-	-	-	-	-
4ASK	-	100%	-	-	-	-	-	-	-
8ASK	-	-	100%	-	-	-	-	-	-
2FSK	-	-	-	0.5%	-	99.5%	-	-	-
4FSK	-	-	-	-	98.25%	1.75%	-	-	-
8FSK	-	-	-	-	-	100%	-	-	-
2PSK	-	-	-	2%	-	98%	-	-	-
4PSK	-	-	-	100%	-	-	-	-	-
8PSK	-	-	-	100%	-	-	-	-	-

TABLE III
N = 2048 WITH NEW THRESHOLDS AND EXTENSION

Digital Modulation Recognition procedure at SNR = 20 dB									
Modulation Type	Deduced Modulation Type								
	2ASK	4ASK	8ASK	2FSK	4FSK	8FSK	2PSK	4PSK	8PSK
2ASK	100%	-	-	-	-	-	-	-	-
4ASK	-	100%	-	-	-	-	-	-	-
8ASK	-	-	100%	-	-	-	-	-	-
2FSK	-	-	-	87%	-	13%	-	-	-
4FSK	-	-	-	-	96.25%	3.75%	-	-	-
8FSK	-	-	-	-	-	100%	-	-	-
2PSK	-	-	-	-	-	100%	-	-	-
4PSK	-	-	-	100%	-	-	-	-	-
8PSK	-	-	-	100%	-	-	-	-	-

TABLE IV
N = 8192 WITH NEW THRESHOLDS AND EXTENSION

Digital Modulation Recognition procedure at SNR = 10 dB									
Modulation Type	Deduced Modulation Type								
	2ASK	4ASK	8ASK	2FSK	4FSK	8FSK	2PSK	4PSK	8PSK
2ASK	100%	-	-	-	-	-	-	-	-
4ASK	-	100%	-	-	-	-	-	-	-
8ASK	-	-	100%	-	-	-	-	-	-
2FSK	-	-	-	100%	-	-	-	-	-
4FSK	-	-	-	-	100%	-	-	-	-
8FSK	-	-	-	-	-	100%	-	-	-
2PSK	-	-	-	-	-	-	100%	-	-
4PSK	-	-	-	-	-	-	-	100%	-
8PSK	-	-	-	-	-	-	-	-	100%

TABLE V
N = 8192 WITH NEW THRESHOLDS AND EXTENSION

Digital Modulation Recognition procedure at SNR = 20 dB									
Modulation Type	Deduced Modulation Type								
	2ASK	4ASK	8ASK	2FSK	4FSK	8FSK	2PSK	4PSK	8PSK
2ASK	100%	-	-	-	-	-	-	-	-
4ASK	-	100%	-	-	-	-	-	-	-
8ASK	-	-	100%	-	-	-	-	-	-
2FSK	-	-	-	100%	-	-	-	-	-
4FSK	-	-	-	-	100%	-	-	-	-
8FSK	-	-	-	-	-	100%	-	-	-
2PSK	-	-	-	-	-	-	100%	-	-
4PSK	-	-	-	-	-	-	-	100%	-
8PSK	-	-	-	-	-	-	-	-	100%

as 8FSK, and 4PSK and 8PSK identified as 2FSK.

We then increase the SNR to 20 dB and re-run the simulation. In this case the simulation results are very similar to the 10 dB case. The only improvement lies in 2FSK, which is now correctly distinguished from 8FSK in 87% of simulations. Additionally, we actually observe a performance decrease in the identification of 4FSK of 2.00%, and all 2PSKs are misidentified as 8FSK.

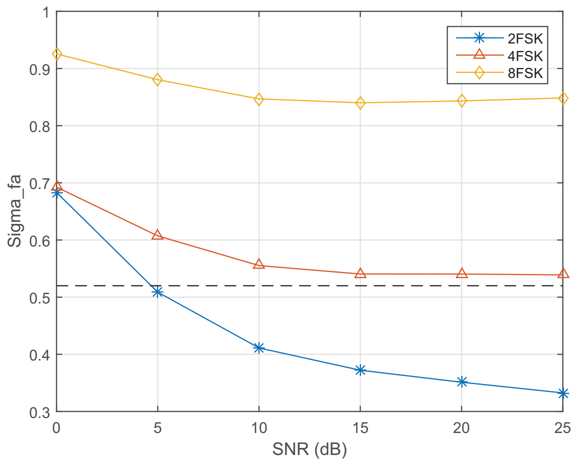

Fig. 5. Dependence of σ_{fa} on SNR (8192).

These results clearly show that an increase in the number of samples is required to properly decode PSK signals.

3) Results with New Thresholds for $N = 8192$: In the next set of simulations, we increase the number of samples to $N = 8192$ and re-run all of the simulations.

This set of stimulations, as shown in Tables IV and V, show the most promising version of our algorithm. At an SNR of 10 dB, all signals are correctly identified in all cases with no errors. This suggests that the biggest driver of sample size will be the proper identification of PSK modulation.

The same is true for an SNR of 20 dB where all signals are also properly identified.

V. Conclusion

In this paper, we have employed five instantaneous features to perform automatic modulation classification and successfully extended previous work to include more modulation types. Once selecting new thresholds as well as increasing the sample size, we are able to achieve 100% classification accuracy.

Acknowledgment

This material is partly based upon work supported by the National Science Foundation under Grant No. 1323240 and No. 1345510, the Air Force Research Laboratory, and the Office of Naval Research. Any opinions, findings, and conclusions or recommendations expressed in this material are those of the author(s) and do not necessarily reflect the views of the funding agencies.

References

[1] B. Ramkumar, "Automatic modulation classification for cognitive radios using cyclic feature detection," *IEEE Transactions on Vehicular Technology*, vol. 9, no. 2, pp. 27–45, 2009.

[2] E. Azzouz and A. Nandi, "Automatic identification of digital modulation types," *Signal Processing*, vol. 47, pp. 55–69, Nov 1995.

[3] W. Wei and J. M. Mendel, "Maximum-likelihood classification for digital amplitude-phase modulations," *IEEE Trans. Commun.*, vol. 48, pp. 189–193, 2000.

[4] K. Kim and A. Polydoros, "Digital modulation classification: the bpsk versus qpsk case," in *Proc. IEEE MILCOM*, pp. 431–436, 1988.

[5] A. Polydoros and K. Kim, "On the detection and classification of quadrature digital modulations in broad-band noise," *IEEE Trans. Commun.*, vol. 38, pp. 1199–1211, 1990.

[6] C. Y. Huang and A. Polydoros, "Likelihood methods for mpsk modulation classification," *IEEE Trans. Commun.*, vol. 43, pp. 1493–1504, 1995.

[7] L. Hong and K. C. Ho, "Classification of bpsk and qpsk signals with unknown signal level using the bayes technique," in *Proc. IEEE ISCAS*, pp. IV.1–IV.4, 2003.

[8] O. A. Dobre, A. Abdi, Y. Bar-Ness, and W. Su, "The classification of joint analog and digital modulations," in *Proc. IEEE MILCOM*, pp. 1–6, 2005.

[9] F. F. Liedtke, "Computer simulation of an automatic classification procedure for digitally modulated communication signals with unknown parameters," *Signal Processing*, vol. 6, pp. 311–323, 1984.

[10] A. K. Nandi and E. E. Azzouz, "Modulation recognition using artificial neural networks," *Signal Processing*, pp. 165–175, 1997.

[11] A. K. Nandi and E. E. Azzouz, "Algorithms for automatic recognition of communication signals," *IEEE Trans. Commun*, vol. 46, pp. 431–436, 1998.

[12] S. Z. Hsue and S. S. Soliman, "Automatic modulation recognition of digitally modulated signals," in *Proc. IEEE MILCOM*, pp. 645–649, 1998.

[13] S. Z. Hsue and S. S. Soliman, "Automatic modulation classification using zero crossing," *IEE Radar and Signal Processing*, vol. vol. 137, pp. 459–464, 1990.

[14] S. Soliman and S. Hsue, "Signal classification using statistical moments," *IEEE Trans. Commun*, vol. 40, pp. 908–9, May 1992.

[15] Y. Qu, X. Li, and Z. Wu, "Software-defined radio based automatic blind hierarchical modulation detector via second-order cyclostationary analysis and fourth-order cumulant," *IEEE Milcom*, 2013.

[16] E. Like, V. Chakravarthy, and Z. Wu, "Modulation recognition in multipath fading channels using cyclic spectral analysis," *IEEE Globecom*, 2008.

[17] E. Like, V. Chakravarthy, Z. Wu, and W. Su, "Modulation recognition in fading channels using higher order cyclic cumulants," *IEEE CrownCom*, 2007.

[18] E. Like, V. Chakravarthy, and Z. Wu, "Reliable modulation classification at low snr using spectral correlation," *IEEE CCNC*, 2007.

[19] J. Herweg, E. Like, V. Chakravarthy, C. Bullmaster, and Z. Wu, "Cyclostationary based classifier for reliable modulation recognition and automated pcr system tuning," *Proceedings 5th Multinational PCR Conference*, 2007.

[20] E. Like, V. Chakravarthy, and Z. Wu, "Signal classification in fading channels using cyclic spectral analysis," *EURASIP Journal on Wireless Communications and Networking*, 2009.

[21] Z. Wu, T. C. Yang, and Z. Liu, "Blind cyclostationary carrier frequency and symbol rate estimation for underwater acoustic communications," *IEEE MMTC E-Letter Special Issue on Acoustic and Audio Communication*, vol. 7, pp. 25–29, February 2012.

[22] X. Li, Q. Han, Z. Liu, and Z. Wu, "Novel modulation detection scheme for underwater acoustic communication signal through short-time detailed cyclostationary features," *IEEE WCNC*, 2014.

[23] Y. Qu, X. Li, and Z. Wu, "Software-defined radio based automatic blind hierarchical modulation detector via second-order cyclostationary analysis and fourth-order cumulant," *IEEE Milcom*, 2013.

[24] J. Sanderson, X. Li, Z. Liu, and Z. Wu, "Hierarchical blind modulation classification for underwater acoustic communication signal via cyclostationary and maximal likelihood analysis," *IEEE Milcom*, 2013.

[25] Z. Wu, T. C. Yang, Z. Liu, and V. Chakarvarthy, "Modulation detection of underwater acoustic communication signals through cyclostationary analysis," *IEEE Milcom*, 2012.

[26] R. Zhou, X. Li, T. Yang, Z. Liu, and Z. Wu, "Real-time cyclostationary analysis for cognitive radio via software defined radio," *IEEE Globecom*, 2012.

[27] Z. Wu and T. C. Yang, "Blind cyclostationary analysis for underwater acoustic communications," *IEEE ICC*, 2012.

[28] Y. Q. HU, J. Liu, and X.-H. Tan, "Digital modulation recognition based on instantaneous information," *The Journal of China Universities of Posts and Telecommunications*, vol. 17, pp. 52–59, June 2010.